Journal of Oral Biology and Craniofacial Research 16 (2026) 101418

Contents lists available at ScienceDirect

Journal of Oral Biology and Craniofacial Research

journal homepage: www.elsevier.com/locate/jobcr

Optimizing graphene-enhanced polycaprolactone scaffolds for bone tissue engineering

Silvia Anitasari [a], Nataniel Tandirogang [b], Hadi Irawiraman [c], Hendrik Setia Budi [d,*], Yung-Kang Shen [e], Levi Natya Alus [f], Prawati Nuraini [g]

[a] Department of Dental Materials and Devices, Faculty of Dentistry, Universitas Mulawarman, Samarinda, 75119, Indonesia
[b] Department of Medical Microbiology, Medical Program, Faculty of Medicine, Universitas Mulawarman, Samarinda, 75119, Indonesia
[c] Department of Anatomical Pathology, Faculty of Medicine, Universitas Mulawarman, Samarinda, 75119, Indonesia
[d] Department of Basic Dental Sciences and Public Health, Oral Biology Division, Faculty of Dental Medicine, Universitas Airlangga, Surabaya, 60132, Indonesia
[e] School of Dental Technology, College of Oral Medicine, Taipei Medical University, Taipei, 11031, Taiwan
[f] Dental Medicine Program, Faculty of Dentistry, Universitas Mulawarman, Samarinda, 75119, Indonesia
[g] Department of Pediatric Dentistry, Faculty of Dental Medicine, Universitas Airlangga, Surabaya, 60132, Indonesia

ARTICLE INFO

Keywords:
Polycaprolactone
Graphene
Scaffold bioactivity
Bone defect
Oral cancer

ABSTRACT

Background: Polycaprolactone (PCL) is widely used in scaffold fabrication due to its biocompatibility and mechanical properties, yet its limited osteoinductive capability hinders effective bone regeneration. To address this, graphene (G) has been incorporated into PCL scaffolds to enhance bioactivity, mechanical strength, and osteogenic potential.
Objective: This study evaluates the osteogenic efficacy of PCL/G composite scaffolds by analyzing osteocalcin (OCN) and osteopontin (OPN) expression and mineralization using Alizarin Red staining.
Methods: Thirty-six adult male rabbits were randomized to four groups and evaluated on day 7, 14 and 21. The PCL/G scaffolds were fabricated using the solvent casting and particle leaching method. A left tibial incision was made and exposing the site for osteotomy. Scaffolds were implanted, and wounds closed. Expression of OCN and OPN were evaluated by immunochemistry and mineralization was evaluated by Alizarin Red staining.
Results: The results indicate that increasing graphene concentration significantly enhances osteogenic activity, with 2.5 wt% graphene demonstrating the highest OCN and OPN expression, as well as superior calcium deposition.
Conclusions: These findings highlight the potential of graphene-based scaffolds in promoting bone regeneration and accelerating clinical translation. Future research should focus on long-term in vivo studies and scaffold degradation kinetics to validate their effectiveness in maxillofacial bone defects due to oral cancer surgery.

1. Introduction

Bone tissue engineering (BTE) offers a transformative alternative to tradtional bone grafting, which is often limited by donor site morbidity, immune rejection, and restricted graft availability.[1] Among the biomaterials used for scaffold fabrication, polycaprolactone (PCL) has gained significant attention due to its biocompatibility, mechanical stability, and ease of processing.[2,3] However, its limited osteoconductive and osteoinductive properties continue to restrict its effectiveness in promoting complete bone regeneration. To overcome these limitation, composite scaffolds incorporating graphene (G) have emerged as a promising strategy. Graphene's exceptional mechanical strength, high surface area, electrical conductivity, and bioactivity enable enhanced osteoblast adhesion, matrix mineralization, and accelerated bone formation.[4]

Despite these advantages, there remains a critical gap in understanding the optimal graphene concentration that maximizes both mechanical reinforcement and osteogenic potential when incorporated into PCL scaffolds.[5] This knowledge is especially important given the increasing prevalence of musculoskeletal disorders and the growing demand for bioengineered bone substitutes in clinical practice. Optimizing PCL/G composite scaffolds could expedite the development of next-generation biomaterials suitable for orthopedic and reconstructive applications.[6]

* Corresponding author.
E-mail address: hendrik-s-b@fkg.unair.ac.id (H.S. Budi).

https://doi.org/10.1016/j.jobcr.2026.101418
Received 27 August 2025; Received in revised form 31 January 2026; Accepted 2 February 2026
Available online 15 February 2026

To address this gap, the present study systematically evaluates the osteogenic performance of PCL/G scaffolds by measuring key bone formation markers-osteocalcin (OCN) and osteopontin (OPN)- and quantifying mineralization through Alizarin Red staining.[6] OCN is a late-stage marker associated with matrix maturation, whereas OPN reflects of three graphene concentration (0.5 wt%, 1.5 wt%, and 2.5 wt%) across multiple time points (day 7, day 14, and day 21), this research aims to identify the graphene content that provides the most favorable osteogenic response.

The objective of this study is to determine the optimal graphene concentration that enhances osteogenic differentiation and mineralization in PCL-based scaffolds, thereby improving their potential for bone defect repair. By elucidating how graphene modulates bone-related marker expression over time, this work advances the development of improved scaffolds with strong translational potential for skeletal tissue engineering.[7]

2. Materials and methods

2.1. Fabrication of PCL/G scaffolds

PCL and PCL/G scaffolds were fabricated using the solvent casting and particle leaching method. PCL (Sigma-Aldrich, Darmstadt, Germany) was dissolved in chloroform (Honeywell, Charlotte, USA) at room temperature for 12 h. The solution was then mixed with varying concentration of graphene and sodium chloride (NaCl; Sigma-Aldrich, Darmstadt, Germany) for 2 h. The graphene was previously prepared by placing a graphite intercalation compound into a preheated crucible at 700^{o}C for 60 s in a standard furnace, located in front of a fume hood to avoid nanoparticle inhalation. Ultrasonication was then used to expand the layers and disperse the graphene in the solvent.

The resulting mixture was poured into a mold and allowed to cure overnight at room temperature. Chloroform was evaporated by placing the cast in vacuum drying oven (Deng Yng, Taipei, Taiwan) at 37 °C for 24 h. To remove the porogen, the scaffolds were washed with deionized (DI) water in a water bath (BH-130D, Taipei, Taiwan), with the water being replaced every 2 h. Finally, the scaffolds were dried in a oven at 50 °C for 12 h.[8,9]

2.2. Preparation of bone defect animal model

2.3. Rabbits were used as animal models due to their suitability for the creation of large bone defects. Animals were kept individually under standard laboratory conditions (25 ± 10 °C; 55 ± 7% humidity) with ad libitum access to food and water. Scaffolds (4x4x4 mm^3) with various graphene ratios were sterilized in 95% ethanol for 24 h, rinsed with 1x PBS, and UV-sterilized for 60 min. Under general anesthesia using 0.35 mL/kg ketamine hydrochloride (Bimeda, Dublin, Ireland), a left tibial incision was made, exposing the site for osteotomy (5x5x1.5 mm) using a surgical burr (Hogy, Jakarta, Indonesia). Scaffolds were implanted, and wounds closed with Vicryl 6-0 sutures (Ethicon, CA, USA). Postoperative monitoring continued under consistent conditions. Euthanasia was performed following imaging on days 7,14, and 2. Tibial sections (5 μm) were analyzed using Immunohistochemistry for OCN and OPN, Alizarin Red S staining, and quantification of OCN and OPN protein expression area, as well as **Alizarin Red S staining area**.[7]

2.3. Immunohistochemistry of OCN and OPN

Paraffin-embedded tissue sections were cut at 5 μm thickness, deparaffinized in xylene, and rehydrated through graded ethanol (100%, 95%, 70%). Slides were rinsed with distilled water, followed by antigen retrieval in 10 mM citrate buffer (pH 6.0) by heating in a water bath at 95 °C for 15–20 min. After cooling to room temperature, slides were rinsed with PBS. Endogenous peroxidase activity was blocked using 3% hydrogen peroxide for 10 min, followed by PBS washing. Non-specific binding was blocked with 5% BSA for 30 min. Slides were incubated overnight at 4 °C with a primary antibody against OCN or OPN (1:100–1:500 dilution). The next day, slides were washed with PBS, and HRP-conjugated secondary antibody was applied for 30–60 min. DAB substrate was used for visualization, producing a brown color indicating positive expression. Slides were rinsed, counterstained with hematoxylin, dehydrated in ethanol, cleared with xylene, mounted, and observed under a light microscope to assess OCN or OPN expression.[6,10]

2.4. Alizarin red S staining

Tissues were washed twice with phosphate-buffered saline (PBS) and fixed in 10% formalin for 15–20 min at room temperature. After rinsing with distilled water, a 1% Alizarin Red S solution (pH 4.1–4.3) was applied for 20–30 min to stain calcium deposits. Excess dye was removed, and tissues were washed thoroughly until background staining was minimal. Samples were observed under a light microscope, where calcium deposits appeared as orange to red areas, indicating positive mineralization and osteogenic activity in the cultured tissues.[8]

2.5. Quantification of OCN and OPN protein expression area

In FIJI software (NIH, USA), images were converted to 8-bit grayscale for analysis. The color deconvolution plugin with the built-in “H DAB” vector was used to separate hematoxylin and DAB channels, with the DAB channel selected for analysis. A threshold was applied to identify positively stained areas, using consistent settings across all images to reduce bias. FIJI then calculated the area fraction (%) of positive staining and the mean gray value (intensity) within the defined region of interest (ROI).[9,11]

2.6. Quantification of alizarin red S staining area

Using FIJI software (NIH, USA), images were converted to 8-bit grayscale and thresholded to select Alizarin Red-stained regions. The "analyze particles" function measured total positive staining area and integrated density. Threshold values and measurement settings were kept consistent across all samples to ensure reliable quantification.[9,12]

2.7. Statistical analysis

All experimental conditions were performed in triplicate (n = 3), and the results are presented as mean ± standard error (SE). Statistical analyses were conducted using OriginPro 2025 software. One-way analysis of variance (ANOVA) was used to compare differences. Prior to performing ANOVA, the data were evaluated for normality and homogeneity of variance to ensure that the assumptions of the test were met. A p-value <0.05 was considered statistically significant.[1]

3. Results

3.1. Osteocalcin (OCN)

At day 7, osteocalcin (OCN) levels are typically lower as osteogenesis is still in its initial phase. The scaffold containing 2.5 wt% G may show slightly higher OCN levels compared to other groups, likely due to improved bioactivity and mechanical reinforcement provided by the graphene content.[13,14] By day 14, osteogenesis progresses, and OCN levels increase. The 2.5 wt% G group is expected to exhibit significantly higher OCN expression, reflecting enhanced osteoblast differentiation and bone matrix deposition. The 1.5 wt% G group may also show a moderate increase in OCN compared to the PCL and 0.5 wt% G.[15]

However by day 21, the formation process reaches more mature stages. The 2.5 wt% G group is anticipated to demonstrate the highest OCN levels, indicating superior bone - regeneration capacity. This result is likely due to better interaction between the graphene and cells,

leading to improved biological compatibility, as shown in Fig. 1A[16]

The quantification of OCN protein expression revealed distinct osteogenic responses across different scaffold groups, including PCL scaffolds and PCL composites incorporated with 0.5 wt%, 1.5 wt%, and 2.5 wt% graphene. OCN is a late stage marker of bone formation, and its increased expression reflects greater maturation of the bone matrix.[17]

In the PCL scaffold group, OCN expression gradually increased from 52.01% on day 7 to 62.83% on day 21. However, this change was not statistically significant ($p = 0.784$), indicating that unmodified PCL scaffolds have limited capacity to stimulate osteoblast differentiation and bone tissue formation.[18]

In contrast, the **0.5 wt% graphene group** demonstrated a statistically significant increase in OCN expression, from 57.54% on day 7 to 96.40% on day 21 ($p = 0.004$). This result indicates that this concentration of graphene effectively enhances osteoblastic activity and promotes osteogenesis.

The **1.5 wt% graphene group** also showed a marked increase in OCN expression, reaching 97.95% by day 21. Although the values were higher than those in the 0.5 wt% group, the changes were not statistically significant ($p = 0.572$), likely due to high variability in the data, as reflected by the large standard error as shown in Fig. 1B.

Similarly, the **2.5 wt% graphene group** exhibited the highest OCN expression, with 120.32% on day 21. However, because the values on day 7 and day 14 were already elevated (92.26% and 92.04%, respectively), the overall increase over time was not statistically significant ($p = 0.256$). This suggests that higher graphene concentrations may elevate OCN expression but could lead to a plateau in biological response, as shown in Table 1.

Table 1
Quantification of OCN protein expression area (%) in PCL and PCL/G scaffold.

Scaffold	Quantification of OCN Protein Expression Area (%)			*p*-value
	Day 7	Day 14	Day 21	
PCL	52.01 ± 16.58	55.22 ± 12.42	62.83 ± 9.65	0.784
0.5 wt% G	57.54 ± 5.84	69.97 ± 3.75	96.40 ± 1.85	0.004[a]
1.5 wt% G	77 ± 13.20	88.24 ± 13.95	97.95 ± 12.90	0.572
2.5 wt% G	92.26 ± 2.50	92.04 ± 2.65	120.32 ± 21.16	0.256

[a] Statistically significant differences were revealed in the 0.5 wt% G on days 7,14, and 21 after implantation.

3.2. Osteopontin (OPN)

The evaluation of osteopontin (OPN) expression in rabbit legs implanted with PCL/G scaffolds demonstrated a clear correlation between graphene demonstrated a clear correlation between graphene concentration and osteogenic activity over time. At day 7, corresponding to the early phase of bone healing, OPN expression was minimal in PCL scaffolds due to their limited bioactivity. In contrast, scaffolds containing graphene exhibited enhanced osteogenesis, with 0.5 wt% G showing moderate OPN expression and 1.5 wt% G and 2.5 wt% G demonstrating significantly higher levels, the latter achieving the strongest response. By day 14, during the mid-stage of bone repair, all graphene-loaded scaffolds displayed substantial improvements in OPN expression compared to PCL, with 1.5 wt% and 2.5 wt% G achieving near-maximal levels. At day 21, representing the late stage of healing, the 2.5 wt% G group maintained the highest and most sustained OPN expression, surpassing all other groups. This consistent trend highlights the superior ability of 2.5 wt% G to stimulate osteogenic activity and promote effective bone regeneration, likely due toits enhanced mechanical properties, surface roughness, and bioactivity,[1,19] which collectively support osteoblast attachment, proliferation, and differentiation. These findings underscore the potential of 2.5 wt% G as the optimal concentration in PCL-based scaffolds for application in bone tissue engineering, as shown in Fig. 2A.

The quantification of **osteopontin (OPN) protein expression** revealed different temporal expression patterns among the scaffold groups, including pure PCL scaffolds and PCL composites containing 0.5 wt%, 1.5 wt%, and 2.5 wt% graphene. OPN is an early-to-mid-stage marker of osteogenesis, playing a crucial role in initial mineral deposition and cell adhesion during bone formation, as shown in Table 3.

Table 2, the **PCL group**, OPN expression was highest at day 7 (62.16%) but decreased sharply over time, reaching 38.17% on day 14 and 34.95% on day 21. Although this trend suggests an early osteogenic response, the decline over time indicates limited sustained activity. The change was not statistically significant ($p = 0.164$). In the **0.5 wt% graphene group**, a similar declining trend was observed, with expression decreasing from 71.41% at day 7 to 51.76% at day 21. While this group maintained relatively higher OPN levels compared to pure PCL at all time points, the overall changes were not statistically significant (p =

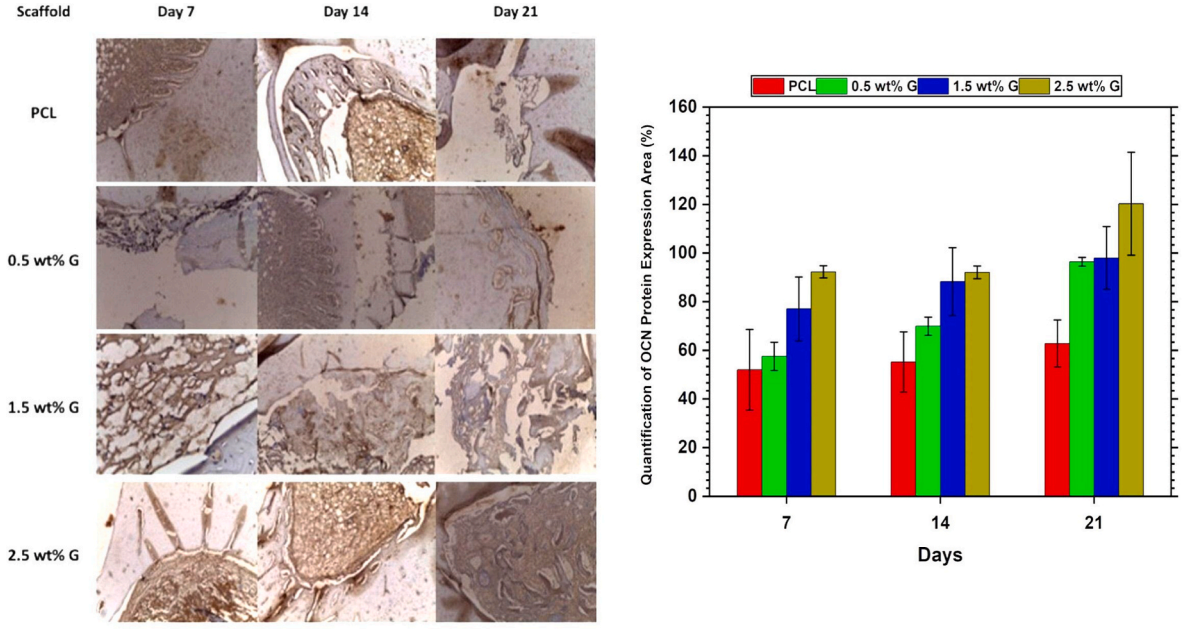

Fig. 1. Immunohistochemical image of OCN staining at day 7, 14, and 21 after implantation.

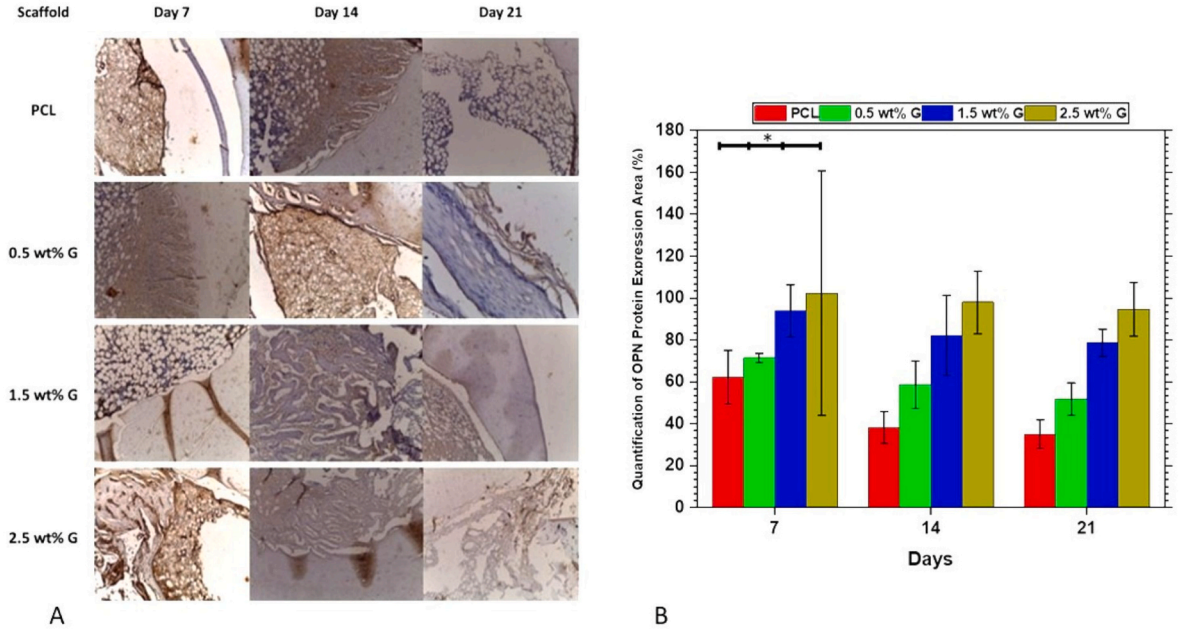

Fig. 2. Immunohistochemical image of OPN staining at day 7, 14, and 21 after implantation.

Table 2
Quantification on OPN protein expression area (%) in PCL and PCL/G scaffold.

Scaffold	Quantification of OPN Protein Expression Area (%)			*p*-value
	Day 7[a]	Day 14	Day 21	
PCL	62.16 ± 12.82	38.17 ± 7.52	34.95 ± 6.79	0.164
0.5 wt% G	71.41 ± 2.01	58.62 ± 11.49	51.76 ± 7.59	0.288
1.5 wt% G	93.85 ± 12.53	82.17 ± 19.09	78.64 ± 6.55	0.727
2.5 wt% G	102.25 ± 58.23	98.02 ± 14.94	94.66 ± 12.69	0.988

[a] Statistical analysis revealed significant differences between PCL and PCL/G scaffolds with various graphene concentrations.

0.288), possibly due to data variability, particularly on day 14. The **1.5 wt% graphene group** exhibited stronger and more consistent OPN expression, starting at 93.85% on day 7 and gradually declining to 78.64% by day 21. Although the standard deviations were relatively large, this group showed sustained osteogenic signaling. However, the changes over time were also not statistically significant ($p = 0.727$). The **2.5 wt% graphene group** showed the highest expression values, peaking at 102.25% on day 7 and slightly declining to 94.66% by day 21. Despite this high expression, the large standard deviation on day 7 (±58.23) contributed to the lack of statistical significance ($p = 0.988$), indicating considerable variability among samples as shown in Fig. 2B.

3.3. Alizarin red staining

On Day 7, for PCL, Alizarin Red staining showed minimal calcium

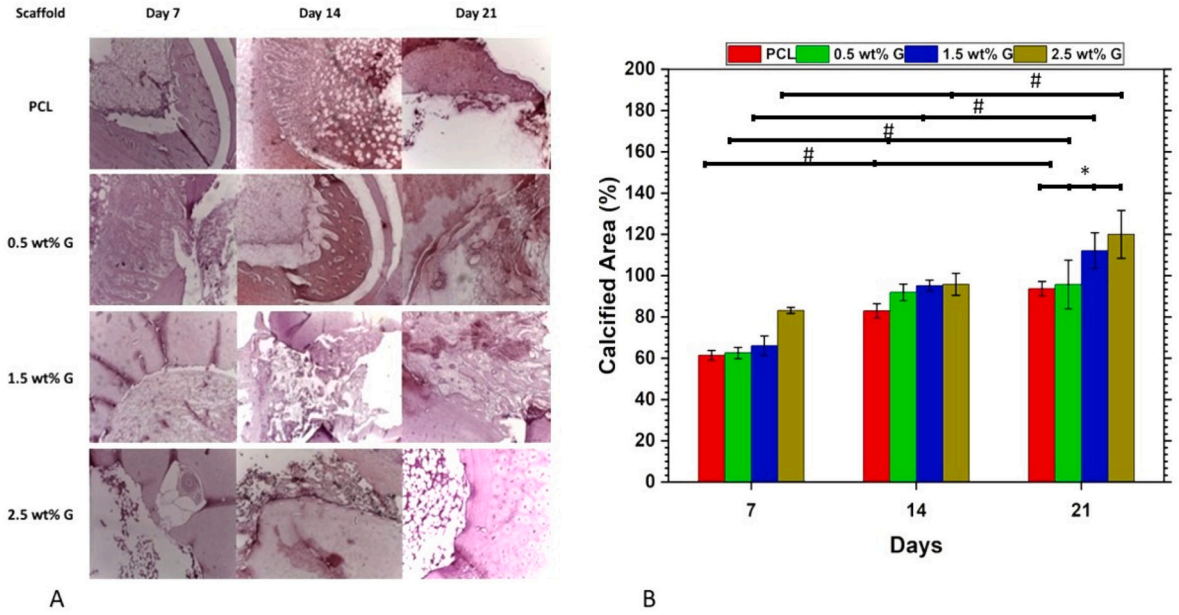

Fig. 3. Alizarin Red Staining at day 7, 14, and 21 after implantation. (For interpretation of the references to color in this figure legend, the reader is referred to the Web version of this article.)

deposition due to limited osteoconductivity and slower bone regeneration. For 0.5 wt% G, the staining was slightly enhanced compared to the PCL, suggesting early stages of mineralization supported by graphene's ability to promote cell adhesion and differentiation. The 1.5 wt% G showed noticeably stronger staining, indicating a significant improvement in calcium deposition due to balanced graphene content enhancing bioactivity. However, the strongest staining was observed with the 2.5 wt% G, which exhibited rapid mineralization and calcium deposition due to higher graphene concentration, as shown in Fig. 3A.[20]

On Day 14, calcium deposition increased for all scaffolds. The PCL showed moderate staining, though it remained weaker than the graphene-containing scaffolds. For 0.5 wt% G, staining was significantly stronger, indicating continued mineralization. The 1.5 wt% G scaffold displayed intense staining, suggesting high calcium deposition and effective osteogenesis due to its balanced bioactivity. The 2.5 wt% G scaffold again showed the best staining, indicating superior calcium deposition and accelerated mineralization at this time point, as shown in Fig. 3A.[21,22]

Table 3 showed the results revealed a progressive increase in the percentage of calcified area over time for all scaffold groups, with a clear enhancement observed as the concentration of graphene increases. The PCL scaffold showed steady mineralization, starting at 61.41% on day 7 and reaching 93.73% by day 21. When 0.5 wt% of graphene was added, calcification improved modestly, with values rising to 95.71% at day 21, indicating a statistically significant increase ($p = 0.036$) compared to the control. A more substantial effect was observed in the 1.5 wt% graphene group, which exhibited enhanced calcification at all time points, culminating in 112.09% by day 21. This suggests that a mid-range graphene concentration may provide optimal conditions for osteogenic activity, with strong statistical significance ($p = 0.004$). The highest concentration tested, 2.5 wt% graphene, resulted in the most rapid and extensive calcification, starting at 83.15% on day 7 and reaching 120% by day 21, again with a statistically significant difference ($p = 0.034$) as shown in Fig. 3B.

4. Discussion

Osteocalcin (OCN) is a late-stage marker of osteoblast differentiation and bone formation. It plays a critical in regulating hydroxyapatite deposition in the bone matrix and contributes to the maturation of minerals. Elevated levels of OCN indicate active bone matrix formation and maturation, which correspond to increased mineral deposition detectable through by Alizarin Red Staining. OCN works in conjunction with osteopontin (OPN) during bone formation; however, its expression typically peaks later than OPN as mineralization progresses.[6,10]

Osteopontin (OPN) is an early-to mid-stage marker of osteogenesis, involved in cell adhesion, signaling, and the initial stages of mineral deposition. It binds to hydroxyapatite and acts as a mediator for mineral-organic interactions in the bone matrix.[23] Elevated OPN expression signifies the onset of mineralization, which can later be visualized using alizarin red staining. While OPN levels may not directly correlate with the extent of mature mineralization, their presence indicates active bone remodeling processes. In the time of osteogenesis, OPN expression precedes OCN. OPN prepares the scaffold for mineral deposition, whereas OCN contributes to the maturation of the mineral matrix.[6,24]

PCL lacks bioactivity to stimulate significant osteogenic differentiation, resulting in low OCN and OPN expression. PCL exhibited weak Alizarin Red Staining due to limited mineralization and poor biological interaction and osteoinduction. Adding 0.5 wt% G slightly improve the slightly improves the scaffold's properties, enhancing osteoblast activity.[25] However, alizarin red staining, initial mineralization occurs but the effects is not optimal due to insufficient graphene content. 1.5 wt% G showed increased OCN and OPN expression, attributed to the synergistic effects of graphene, including enhanced mechanical and electrical properties. This group showed stronger Alizarin resd staining, reflecting more robust mineralization and calcium deposition.[26,27]

The 2.5 wt% G showed the highest OCN and OPN expression, as the optimal graphene content supported both early and late stages of osteogenesis. This group exhibited intense Alizarin Red staining, indicating high calcium deposition and substantial mineralized matrix formation, which reflected superior bone regeneration. The enhanced biological properties of 2.5 wt% G improved the scaffold's ability to mimic the native bone environment, promoting cell adhesion, proliferation, and differentiation. It when enhanced graphene content improves the scaffold's ability to mimic the native bone environment, promoting cell adhesion, proliferation, and differentiation.[28,29] The high graphene concentration ensured structural stability, supporting osteogenesis under physiological conditions. Furthermore, graphene facilitated bioelectrical signaling, a critical factor for osteoblast differentiation, contributing to the scaffold's superior performance in promoting bone regeneration.[2,30]

Despite the promising findings, several limitation should be acknowledged. (1) This study evaluated osteogenic markers (OPN and OCN) at selected time points only, which may not fully capture the dynamic progression of osteogenesis across earlier or later stages. (2). This study did not evaluate long-term degradation behavior of the PCL/G scaffold, which is essential for understanding scaffold-tissue interactions in vivo. (3) The use of the tibial bone defect model, while providing accessibility and adequate size for scaffold evaluation, may not fully replicate the anatomical and functional characteristics of jaw (maxillofacial) bone, and this should be considered a limitation when extrapolating results to clinical applications. (4) Finally, the findings are based on in vitro analysis only, and the osteogenic response in vivo may vary due to the complexity of biological environments, mechanical loading, and immune interactions.

Table 3
Calcified Area (%) in PCL and PCL/G scaffold.

Scaffold	Calcified Area (%)			*p*-value
	Day 7	Day 14	Day 21[a]	
PCL	61.41 ± 2.38	82.95 ± 3.49	93.73 ± 3.52	0.001[b]
0.5 wt% G	62.53 ± 2.78	91.93 ± 4.01	95.71 ± 11.75	0.036[b]
1.5 wt% G	66.05 ± 4.75	95.22 ± 2.66	112.09 ± 8.70	0.004[b]
2.5 wt% G	83.15 ± 1.45	95.83 ± 5.31	120 ± 11.64	0.034[b]

[a] Significant differences between PCL and various concentration of PCL/G scaffolds on day 21.

[b] Significant differences between PCL and various concentration of PCL/G on days 7, 14, and 21.

5. Conclusion

This study demonstrates the potential of graphene-enhanced PCL scaffolds for bone tissue engineering. Increasing graphene concentration improved osteogenic activity, with 2.5 wt% graphene showing the highest bioactivity and mineralization. These findings suggest that optimizing graphene content can enhance scaffold performance for bone regeneration. Nevertheless, future studies are required to evaluate long-term in vivo effects, particularly regarding biodegradation and bone remodeling balance, as well as to explore clinical translation to establish graphene-based scaffolds as a viable approach for bone defect repair.

Patient's/Guardian's consent

This study did not involve human participants, and therefore, informed consent were not required.

Ethical clearance

This study received ethical approval from the Faculty of Medicine, Mulawarman University (No.191/KEPK-FK/VII/2024). All procedures followed institutional guidelines for the care and use of laboratory

animals and complied with the National Guidelines for the Care and Use of Laboratory Animals in Indonesia and the internationally accepted principles for laboratory animal use and care.

Patients guardians consent

We declared that no humans were used as patients in our study. We used animal model for bone defect following the ethical clearance. This study received ethical approval from the Faculty of Medicine, Mulawarman University (No.191/KEPK-FK/VII/2024).

Source of funding

We declared that no financial support for the research.

Declaration of competing interest

The authors declare that they have no known competing financial interests or personal relationships that could have appeared to influence the work reported in this paper.

Acknowledgement

We would like to express our sincere gratitude to Universitas Mulawarman, Universitas Airlangga, and Taipei Medical University for their invaluable support and collaboration in this research endeavor.

Data availability

The data used to support the finding of this research are included in the article.

References

1. Budi H, Anitasari S, Shen Y, Yamada S. Cytoskeletal regulation on polycaprolactone/graphene porous scaffolds for bone tissue engineering. *Sci Rep*. 2024;14.
2. Sadek A, Elkareem M, Abdelhamid H, Moustafa S, Hussein K. Repair of critical-sized bone defects in rabbit femurs using graphitic carbon nitride (g-C3N4) and graphene oxide (GO) nanomaterials. *Sci Rep*. 2023;13.
3. Govindarajan D, Saravanan S, Sudhakar S, Vimalraj S. Graphene : a multifaceted carbon-based material for bone tisue engineering applications. *ACS Omega*. 2024;9:67–80.
4. Anitasari S, Wu C, YK S. PCL/Graphene scaffolds for the osteogenesis process. *Bioengineering*. 2023;10:305.
5. Wang Q, Yang X, Wang G, et al. Osteogenic growth peptide-loaded 3D-printed PCL scaffolds for the promotion of osteogenesis through the ERK pathway. *Mater Des*. 2020;193.
6. Vancea A, Serban O, Fodor D. Relationship between osteopontin and bone mineral density. *Acta Endocrinol*. 2021;17:509–516.
7. Lopes-Nalesso P, Wang W, Hou Y, et al. In vivo investigation of 3D printed polycaprolactone/graphene electro-active bone scaffolds. *Bioprinting*. 2021;24.
8. Bernar A, Gebetsberger J, Bauer M, Streif W, Schirmer M. Optimization of the alizarin red S assay by enhancing mineralization of osteoblasts. *Int J Mol Sci*. 2022;24:723.
9. Zareian R, Kheradvar A. *Method for Identification and Quantification of Tissue Calcification*. 2020.
10. Hosseini S, Naderi-Manesh H, Vali H, et al. Contribution of osteocalcin-mimetic peptide enhances osteogenic activity and extracellular matrix mineralization of human osteoblast-like cells. *Colloids Surf B Biointerfaces*. 2019;1:662–671.
11. Crowe A, Yue W. Semi-quantitative determination of protein expression using immunohistochemistry staining and analysis: an integrated protocol. *Bio Protoc*. 2019;9.
12. Li X, Chan Y, Jiang Y. Development of an image processing software for quantification of histological calcification staining images. *PLoS One*. 2023;18.
13. Tian J, Li D, Zhang F, Feng H, Sun W. Construction and performance evaluation of polycaprolactone/nanodiamond-phospholipid composite materials. *CJTER*. 2025;29:3380–3387.
14. Yang Y, He H, Miao F, et al. 3D-printed PCL framework assembling ECM-Inspired multi-layer mineralized GO-Col-HAp microscaffold for in situ mandibular bone regeneration. *J Transl Med*. 2024;22.
15. Zhang X, Li L, Li S, Liang J, Chen F, Yin Y. Preparation and biological characteristics of extracellular matrix vesicle mimetics. *Chin J Stomatol*. 2024;59:663–671.
16. Kashte S, Kadam S, Maffulli N, Potty A, Migliorini F, Gupta A. Osteoinductive potential of graphene and graphene oxide for bone tissue engineering: a comparative study. *J Orthop Surg Res*. 2024;19:527.
17. Amiryaghoubi N, Fathi M, Barzegari A, Barar J, Omidian H, Omidi Y. Recent advances in polymeric scaffolds containing carbon nanotube and graphene oxide for cartilage and bone regeneration. *Mater Today Commun*. 2021;26.
18. Banimohamad-shotorbani B, Rahmani Del Bakhshayesh A, Mehdipour A, Jarolmasjed S, Shafaei H. The efficiency of PCL/HAp electrospun nanofibers in bone regeneration: a review. *J Med Eng Technol*. 2021;45:511–531.
19. Anitasari S, Wu C, Shen Y. PCL/Graphene scaffolds for the osteogenesis process. *Bioengineering*. 2023;10.
20. Mc Ginty J, Yazdanpanah N, Price C, Ter Horst JHJS. *Nucleation and crystal growth. In: Continuous Crystallization (Chapter 1)*. 2020:1–20. *RSC*.
21. Anitasari S, Belem W, Wahab D. The effect of hydroxyapatite on alveolar bone regeneration in various dental procedure: syatematic review and meta-analysis. *Amplitudo*. 2024;3:15–20.
22. Bobbert F, Zadpoor A. Effects of bone substitute architecture and surface properties on cell response, angiogenesis, and structure of new bone. *RSC*. 2017;5:6175–6192.
23. Illine-Vul T, Raju N, Mateos B, et al. Osteopontin regulates biomimetic calcium phosphate crystallization from disordered mineral layers covering apatite crystallites. *Sci Rep*. 2020;10.
24. Depalle B, McGilvery C, Nobakhti S, Aldegaither N, Shefelbine S, Porter A. Osteopontin regulates type I collagen fibril formation in bone tissue. *Acta Biomater*. 2021;120:194–202.
25. Feng P, Zhao R, Tang W, et al. Structural and functional adaptive artificial bone: materials, fabrications, and properties. *Adv Funct Mater*. 2023;33.
26. Antunovic F, Tolosa F, Klein C, Ocaranza R. Polycaprolactone-based scaffolds for guided tissue regeneration in periodontal therapy: a systematic review. *J Appl Biomater Funct Mater*. 2023;21.
27. Si J, Wang C, Zhang D, Wang B, Hou W, Zhou Y. Osteopontin in bone metabolism and bone diseases. *Med Sci Monit*. 2020;26. e919159-919151–e919159-919159.
28. Duda G, Geissler S, Checa S, Tsitsilonis S, Petersen A, Schmidt-Bleek K. The decisive early phase of bone regeneration. *Nat Rev Rheumatol*. 2023;19:78–95.
29. Jeong JT, Choi MK, Sim Y, et al. Effect of graphene oxide ratio on the cell adhesion and growth behavior on a graphene oxide-coated silicon substrate. *Sci Rep*. 2016;6,33835.
30. Tang M, Xu K, Shang H, et al. Biomineralization of bone-like hydroxyapatite to upgrade the mechanical and osteoblastic performances of poly(lactic acid) scaffolds. *Int J Biol Macromol*. 2023;226:1273–1283.